Selective Suppression of Cellular Immunity and Increased Cytotoxicity in Skin Lesions of Disseminated Leishmaniasis Uncovered by Transcriptome-Wide Analysis

Journal of Investigative Dermatology (2021) **141,** 2542–2546; doi:10.1016/j.jid.2021.03.017

TO THE EDITOR

Disseminated leishmaniasis (DL) is an emerging form of cutaneous leishmaniasis (CL) where multiple acneiform or papular lesions occur at ≥2 noncontiguous anatomical regions affecting various body segments (Costa et al., 1986). With increasing incidence in endemic areas of *Leishmania braziliensis* transmission, DL is a difficult-to-treat disease owing to the elevated number of lesions, the frequent mucosal involvement, and the low cure rate (Machado et al., 2019). Lack of lymph node enlargement and the rapid spread of lesions to many parts of the skin and mucosa suggest that the parasites disseminate through the bloodstream (Costa et al., 1986), and both host and parasite factors have been implicated in this manifestation. Patients with DL exhibit an in situ response characterized by IFN-γ, TNF, IL-10, TGFβ, CCL2, CCL3, and CXCL10, with levels similar to those observed in localized CL (LCL) lesions (Machado et al., 2011). However, the host response in DL has so far only been studied using limited cytokine panels, and more comprehensive studies are needed.

To investigate the transcriptome-wide in situ response in DL, we employed RNA sequencing of lesion biopsies (n = 7) and compared them with unrelated healthy skin controls (n = 4); institutional approval for the experiments and written informed patient consent were obtained (Supplementary Table S1 and Supplementary Material and Methods). A total of 2,149 differentially expressed genes were identified in this comparison (Supplementary Table S2), the majority of which were upregulated (1,765 genes), whereas only 384 were found to be downregulated (Supplementary Figure S1). Enrichment analysis of these differentially expressed genes was performed, and a total of 49 processes were found to be upregulated, whereas 8 processes were downregulated (Supplementary Figure S2a). Collectively, these results indicate that gene expression in DL is geared toward the activation of tissue remodeling pathways, with concomitant dampening of the cellular immune response, a hallmark of LCL (Supplementary Figure S2a and b). We then further explored which markers of the immune response characterized this observed deregulation, with respect to the relevance of $CD4^+$ T cells and IFN-γ in controlling *Leishmania* infection (reviewed in Novais and Scott [2015]). In general, transcripts coding for inflammatory cytokines, including IL-1B and IL-6, were more expressed in DL lesions than in controls, whereas *LTA* and *TNF* were downregulated (Figure 1a). Of note, the expression of *IFNG* did not reach statistical significance compared with that in the controls, although it was found more expressed in some of the lesions (log_2-fold change = 2.66; false discovery rate = 0.12) (Figure 1a). Strikingly, chemokines and markers of cytotoxicity were strongly upregulated, which is consistent with the observed enrichment of biological processes related to cell chemotaxis and inflammatory response (Supplementary Figure S2a). On examination of the number of transcripts expressed by each patient, the significantly higher expression of *IL10* (associated with parasite persistence), confirmed by immunohistochemical staining, in parallel with markedly lower expression of *IL13*, *LTA*, *TNF*, and *TGFB1* were notable (Figure 1b and e). Variability in the expression of *IFNG* and *IL10* has been reported in previous transcriptomic studies using lesions, with *IFNG* ranging between 3.12 and 8.29 and *IL10* ranging within 0.5–4.54 (log_2fold change vs. controls) in LCL datasets (Amorim et al., 2019; Christensen et al., 2016; Novais et al., 2015; Rodrigues et al., 2019). Thus, the expression profiles of *IFNG* and *IL10* identified in DL lesions lay within the lower range of expression than that of LCL forms. Of note, diffuse CL (DCL) also presents with lowered *IFNG* production in situ that together with other unique features of this manifestation, which also involves parasite spread, could be associated with a shift from T helper (Th)1 responses impairing a proper host immune defense (Christensen et al., 2019). As expected, the number of transcripts coding for chemokines was significantly higher in DL lesions than in the controls (Figure 1c). Finally, we observed a significant increase in *GZMA*, a T- and NK-cell–specific serine protease associated with cytotoxic response. Other mediators of cytotoxicity were also significantly upregulated in the DL lesions: *CTSB*, *GZMH*, *CTSC*, and *FASLG* (Supplementary Table S2). The notion of an impaired type 1 immune response in patients with DL was previously proposed on the basis of the low expression of IFN-γ and TNF-α in PBMC (Leopoldo et al., 2006; Machado et al., 2011), but no differences in their in situ production were observed between DL and LCL samples by Machado et al. (2011). Importantly, the Th1/Th2 paradigm observed in experimental infection models, in which the

Abbreviations: CL, cutaneous leishmaniasis; DCL, diffuse cutaneous leishmaniasis; DL, disseminated leishmaniasis; LCL, localized cutaneous leishmaniasis; Th, T helper

Accepted manuscript published online 3 April 2021; corrected proof published online 21 May 2021

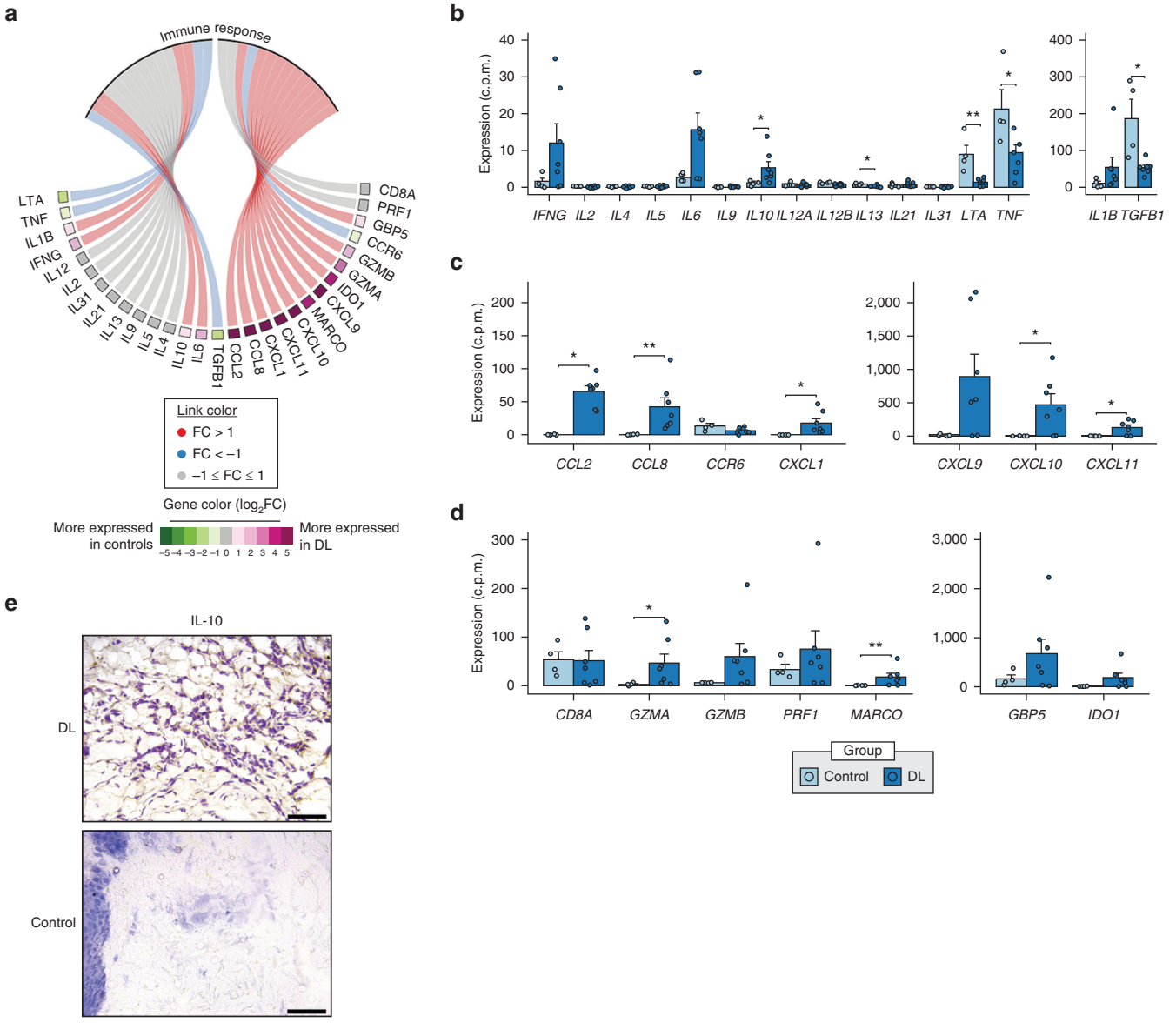

Figure 1. Bird's-eye view of the modulation of selected immune-related genes in DL lesions. (**a**) Circular plot linking immune response processes with corresponding gene expression. Link colors indicate more (red) or less (blue) expression in DL than in the controls or no gene modulation (gray). The color of nodes near gene labels reflects $\log_2$-transformed FC values. Differentially expressed genes appear bolded. (**b**–**d**) Normalized expression values of genes that appear in panel **a**. Data are expressed as mean ± SEM for n = 7 (DL group) and n = 4 (control group) individuals, with individual data points overlaid. DL and control groups were compared using the Mann–Whitney *U* test. $*P < 0.05$, $**P < 0.01$. The representative transcripts analyzed in this study were obtained from a previous study (Christensen et al., 2019) and the references in it. (**e**) Immunostaining of IL-10 in a tissue sample from DL lesion and normal skin obtained from plastic surgery. Magnification: ×40, bar = 50 μm. c.p.m., counts per million; DL, disseminated leishmaniasis, FC, fold change.

first associates with cure and the latter associates with disease progression (Sacks and Noben-Trauth, 2002), does not fully capture the multiple facets of the disease in humans, which is characterized by stark heterogeneity in clinical presentations and, not uncommonly, by mixed Th1/Th2 immune responses. Collectively, these results strengthen and expand the notion that selective immunosuppression, coupled with activation of cytotoxic molecules, is present in DL lesions.

Next, we compared the transcriptome-wide signature between DL and previously published lesion transcriptomes of patients with LCL (Christensen et al., 2016; Novais et al., 2015) and DCL (Christensen et al., 2019). In DCL, pathogen spread is accompanied by an abundance of parasites (contrary to DL), and patients are refractory to treatment (Silveira et al., 2004). Gene Set Enrichment Analysis analysis using MSigDB as a template disclosed unique and/or shared pathways among these forms, six of which are common to all conditions, 25 being DL specific (Figure 2). Identified in the core response are pathways related to inflammation, a prominent feature of tegumentary leishmaniasis, whereas processes related to signaling, development, and proliferation were exclusively recognized in DL, including MYC targets; the p53 pathway; signaling by KRAS, hedgehog, and TGFβ; as well as angiogenesis (Figure 2), in support of previous findings suggesting a role for

Figure 2. Conserved and shared transcriptional patterns across the spectrum of tegumentary leishmaniasis. GSEA was performed for available expression data of lesions of three clinical forms of CL: DL (this work), DCL (Christensen et al., 2019), and LCL (Christensen et al., 2016; Novais et al., 2015). Circles represent the activated hallmark gene sets (NES > 0) in the comparison of infected with healthy skin for each dataset, with radii proportional to NES. Circle colors represent FDR-corrected *P*-values for each term, with gray-colored circles indicating terms that had FDR > 0.05, although enriched in a given dataset. Hallmark processes were considered shared between LCL and other clinical forms when significantly enriched in at least one LCL dataset. Akt, protein kinase B; CL, cutaneous leishmaniasis; DCL, diffuse cutaneous leishmaniasis; DL, disseminated leishmaniasis; FDR, false discovery rate; GSEA, Gene Set Enrichment Analysis; LCL, localized cutaneous leishmaniasis; NES, normalized enrichment score; ns, not significant; PI3K, phosphatidylinositol 3 kinase; STAT, signal transducer and activator of transcription.

vessel proliferation to parasite survival and growth in DL (Mendes et al., 2013). These multiple biological processes potentially contribute to driving more research dissecting the basis of parasite dissemination in this clinical manifestation.

To explore the population of cells that could be involved in the immune landscape described earlier, digital cytometry (Finotello et al., 2019) was performed using RNA sequencing data as input. DL lesions were characterized by the presence of neutrophils (11.1 ± 4.1%; mean ± SD of quanTIseq-predicted cell fractions), NK cells (6.1 ± 1.7%), and M1 (13.6 ± 8.4%) and M2 (3.1 ± 2.0) macrophages (Supplementary Figure S3a). Other cell populations were also detected, such as $CD4^+$ and $CD8^+$ T cells and B cells, albeit with variability that likely reflects interspecimen heterogeneity. For instance, the estimated abundance of B cells in one patient was 29% (range: 3−29%; mean ± SD of 7 ± 10%). Coincidently, the two patients who presented the highest proportions of B cells (29% and 8%) also had mucosal involvement. Previously reported evidence in human CL forms caused by *L. braziliensis* showed that overexpression of B-cell transcripts occurs to varying degrees in the lesions (Amorim et al., 2019; Christensen et al., 2019), and B cells were also identified in DL lesions (Mendes et al., 2013). Taken together, our findings suggest that DL lesions can be characterized by an inflammatory signature in which chemokines, neutrophils, and macrophages are strongly present, in addition to cytotoxic markers and NK cells. To assess the differences in the immune infiltrate composition across various CL manifestations, we also compared the prediction of the immune infiltrate of DL lesions with those of DCL and LCL. These results revealed unique patterns of each disease (Supplementary Figure S3a) as well as marked variability within CL presentations (Supplementary Figure S3b). Notably, DL and DCL presented with significantly lower estimates of M1 macrophages in situ, and these classically activated macrophages are usually associated with *Leishmania* clearance (Christensen et al., 2019). The presence of $CD4^+$ and $CD8^+$ cells was confirmed by immunohistochemistry in independent samples of DL and LCL lesions, with DL presenting a weaker signal of both T-cells subsets (Supplementary Figure S3c). Decreased $CD8^+$ cell fractions were also detected in DL samples compared with those in LCL (Supplementary Figure S3a), but this was not statistically supported. However, lower fractions of $CD8^+$ in DCL samples, which we verified using digital cytometry (Supplementary Figure S3a), have also been reported in the literature (Hernández-Ruiz et al., 2010). In humans, recruitment of granzyme-producing $CD8^+$ T cells to lesions is associated with CL severity while also contributing to tissue damage in cutaneous lesions caused by *L. braziliensis* (Brodskyn et al., 1996; Santos et al., 2013). In mice, cytotoxic T cells promote metastatic lesions (Novais et al., 2013). If further studies confirm a lower number of $CD8^+$ T cells in DL lesions, this could point to NK cells as a source of cytotoxicity (Berke, 1995), a finding recently reported in the PBMCs of patients with aggravated LCL (Campos et al., 2020).

Our study presents possibilities and limitations of the transcriptome-wide analysis of human CL lesions. Particularly, our unpaired study design is unable to fully account for individual-level variations in gene expression, which could be overcome by a paired design with control samples deriving from healthy and preferably comparable skin segments of the same subject, yielding an improved statistical power. However, bioethical concerns in performing a punch biopsy in the healthy skin of a patient prompted us to employ alternative control skin obtained from surgical discards of individuals undergoing elective procedures. Although our limited sample size narrows the ability to draw definitive conclusions, particularly concerning the prediction of cellular populations in DL lesions, we were able to validate in silico predictions of T-cells subsets by immunohistochemistry.

In summary, this analysis revealed that DL is a manifestation that differs from other CL forms clinically and also at the gene expression level. Our results not only highlighted the similarities across the spectrum of human CL but also revealed specific markers to each clinical form, which may ultimately be reflected by differences in host gene expression levels during active disease. Functional studies are warranted to follow up on some of the unique molecular pathways identified in this work, contributing to an enhanced comprehension of the mechanisms by which parasite dissemination occurs in DL and how to prevent it.

Data availability statement

Datasets related to this article can be found in National Center for Biotechnology Information's Sequence Read Archive (Leinonen et al., 2011) and are accessible through BioProject accession PRJNA576449.

ORCIDs

Pablo Ivan Pereira Ramos: http://orcid.org/0000-0002-9075-7861
Juqueline Rocha Cristal: http://orcid.org/0000-0002-6816-6846
Ricardo Khouri: http://orcid.org/0000-0001-5664-4436
Viviane Boaventura: http://orcid.org/0000-0002-7241-6844
Lucas Gentil Azevedo: http://orcid.org/0000-0003-1873-5956
Thaizza Cavalcante Correia: http://orcid.org/0000-0002-3264-9977
Rohit Sharma: http://orcid.org/0000-0002-2195-3623
Cristina R. de Barros Cardoso: http://orcid.org/0000-0002-6156-3144
Camila Figueiredo Pinzan: http://orcid.org/0000-0001-7635-2107
Almério Libório Lopes de Noronha: http://orcid.org/0000-0002-1312-8156
Johan Van Weyenbergh: http://orcid.org/0000-0003-3234-8426
Artur Trancoso Lopo de Queiroz: http://orcid.org/0000-0003-4908-9993
Camila I. de Oliveira: http://orcid.org/0000-0002-7868-5164
Manoel Barral-Netto: http://orcid.org/0000-0002-5823-7903
Aldina Barral: http://orcid.org/0000-0002-7177-464X

CONFLICT OF INTEREST

The authors state no conflict of interest.

ACKNOWLEDGMENTS

AB, CIDO, CRDBC, and MBN are fellows from the Brazilian National Research Council (CNPq). Funding from Fundação Oswaldo Cruz is acknowledged by ATLDQ (INOVA - Process VPPIS-001-FIO-18-45) and VB (INOVA - Process VPPCB-007-FIO-18-2-4). LGA is supported by a scholarship from Fundação de Amparo à Pesquisa da Bahia. This study was financed in part by the Coordenação de Aperfeiçoamento de Pessoal de Nível Superior — Brazil (finance code 001) and the Research Foundation - Flanders (Brussels, Belgium) (grant G0D6817N). The authors gratefully acknowledge Andris K. Walter for English language revision and manuscript copyediting assistance.

AUTHOR CONTRIBUTIONS

Conceptualization: AB, MBN; Formal Analysis: ATLDQ, JRC, LGA, PIPR, RK; Funding Acquisition: AB, MBN; Methodology: ALLDN, RK, TCC, VB, CRDBC, CFP, JRC, JVW, RS; Supervision: AB; Visualization: PIPR; Writing — Original Draft Preparation: CIDO, PIPR; Writing — Review and Editing: AB, CIDO, JVW, MBN, PIPR, VB

Disclaimer
The funders had no role in study design, data collection and analysis, decision to publish the study, or the preparation of the manuscript.

***Pablo Ivan Pereira Ramos*[1,7,*], *Juqueline Rocha Cristal*[1,7], *Ricardo Khouri*[1,2], *Viviane Boaventura*[1], *Lucas Gentil Azevedo*[1], *Thaizza Cavalcante Correia*[1], *Rohit Sharma*[1], *Cristina R. de Barros Cardoso*[3], *Camila Figueiredo Pinzan*[3,4], *Almério Libório Lopes de Noronha*[5], *Johan Van Weyenbergh*[2], *Artur Trancoso Lopo de Queiroz*[1], *Camila I. de Oliveira*[1,6,8], *Manoel Barral-Netto*[1,6,8] and *Aldina Barral*[1,6,8]**

[1]*Instituto Gonçalo Moniz, Fundação Oswaldo Cruz (FIOCRUZ), Salvador, Brazil;* [2]*Department of Microbiology and Immunology, Rega Institute for Medical Research, Clinical and Epidemiological Virology, KU Leuven, Leuven, Belgium;* [3]*Department of Clinical Analysis, Toxicology and Food Sciences, School of Pharmaceutical Sciences of Ribeirão Preto, University of São Paulo (USP), Ribeirão Preto, Brazil;* [4]*Department of Biochemistry and Immunology, Ribeirão Preto Medical School, University of São Paulo (USP), Ribeirão Preto, Brazil;* [5]*Laboratório de Anatomia Patológica, Feira de Santana, Brazil; and* [6]*Instituto de Investigação em Imunologia (iii-INCT), São Paulo, Brazil*
[7]*These authors contributed equally to this work.*
[8]*These authors contributed equally as senior authors.*
[*]*Corresponding author e-mail: pablo.ramos@fiocruz.br*

SUPPLEMENTARY MATERIAL

Supplementary material is linked to the online version of the paper at www.jidonline.org, and at https://doi.org/10.1016/j.jid.2021.03.017.

REFERENCES

Amorim CF, Novais FO, Nguyen BT, Misic AM, Carvalho LP, Carvalho EM, et al. Variable gene expression and parasite load predict treatment outcome in cutaneous leishmaniasis. Sci Transl Med 2019;11:eaax4204.

Berke G. Unlocking the secrets of CTL and NK cells. Immunol Today 1995;16:343–6.

Brodskyn CI, Barral A, Bulhões MA, Souto T, Machado WC, Barral-Netto M. Cytotoxicity in patients with different clinical forms of Chagas' disease. Clin Exp Immunol 1996;105:450–5.

Campos TM, Novais FO, Saldanha M, Costa R, Lordelo M, Celestino D, et al. Granzyme B produced by natural killer cells enhances inflammatory response and contributes to the immunopathology of cutaneous leishmaniasis. J Infect Dis 2020;221:973–82.

Christensen SM, Dillon LA, Carvalho LP, Passos S, Novais FO, Hughitt VK, et al. Meta-transcriptome profiling of the human-Leishmania braziliensis cutaneous lesion [published correction appears in PLoS Negl Trop Dis 2017;11:e0005588]. PLoS Negl Trop Dis 2016;10:e0004992.

Christensen SM, Belew AT, El-Sayed NM, Tafuri WL, Silveira FT, Mosser DM. Host and parasite responses in human diffuse cutaneous leishmaniasis caused by L. amazonensis. PLoS Negl Trop Dis 2019;13:e0007152.

Costa JM, Marsden PD, Llanos-Cuentas EA, Netto EM, Carvalho EM, Barral A, et al. Disseminated cutaneous leishmaniasis in a field clinic in Bahia, Brazil: a report of eight cases. J Trop Med Hyg 1986;89:319–23.

Finotello F, Mayer C, Plattner C, Laschober G, Rieder D, Hackl H, et al. Molecular and pharmacological modulators of the tumor immune contexture revealed by deconvolution of RNA-seq data. Genome Med 2019;11:34.

Hernández-Ruiz J, Salaiza-Suazo N, Carrada G, Escoto S, Ruiz-Remigio A, Rosenstein Y, et al. CD8 cells of patients with diffuse cutaneous leishmaniasis display functional exhaustion: the latter is reversed, in vitro, by TLR2 agonists. PLoS Negl Trop Dis 2010;4:e871.

Leinonen R, Sugawara H, Shumway M, International Nucleotide Sequence Database Collaboration. The sequence read archive. Nucleic Acids Res 2011;39(Suppl_1):D19–21.

Leopoldo PT, Machado PR, Almeida RP, Schriefer A, Giudice A, de Jesus AR, et al. Differential effects of antigens from L. braziliensis isolates from disseminated and cutaneous leishmaniasis on in vitro cytokine production. BMC Infect Dis 2006;6:75.

Machado GU, Prates FV, Machado PRL. Disseminated leishmaniasis: clinical, pathogenic, and therapeutic aspects. An Bras Dermatol 2019;94:9–16.

Machado PR, Rosa ME, Costa D, Mignac M, Silva JS, Schriefer A, et al. Reappraisal of the immunopathogenesis of disseminated leishmaniasis: in situ and systemic immune response. Trans R Soc Trop Med Hyg 2011;105:438–44.

Mendes DS, Dantas ML, Gomes JM, Santos WL, Silva AQ, Guimarães LH, et al. Inflammation in disseminated lesions: an analysis of CD4+, CD20+, CD68+, CD31+ and vW+ cells in non-ulcerated lesions of disseminated leishmaniasis. Mem Inst Oswaldo Cruz 2013;108:18–22.

Novais FO, Carvalho LP, Graff JW, Beiting DP, Ruthel G, Roos DS, et al. Cytotoxic T cells mediate pathology and metastasis in cutaneous leishmaniasis. PLoS Pathog 2013;9:e1003504.

Novais FO, Carvalho LP, Passos S, Roos DS, Carvalho EM, Scott P, et al. Genomic profiling of human Leishmania braziliensis lesions identifies transcriptional modules associated with cutaneous immunopathology. J Invest Dermatol 2015;135:94–101.

Novais FO, Scott P. CD8+ T cells in cutaneous leishmaniasis: the good, the bad, and the ugly. Semin Immunopathol 2015;37:251–9.

Rodrigues V, André S, Maksouri H, Mouttaki T, Chiheb S, Riyad M, et al. Transcriptional analysis of human skin lesions identifies tryptophan-2,3-deoxygenase as a restriction factor for cutaneous Leishmania. Front Cell Infect Microbiol 2019;9:338.

Sacks D, Noben-Trauth N. The immunology of susceptibility and resistance to Leishmania major in mice. Nat Rev Immunol 2002;2:845–58.

Santos Cda S, Boaventura V, Ribeiro Cardoso C, Tavares N, Lordelo MJ, Noronha A, et al. CD8(+) granzyme B(+)-mediated tissue injury vs. CD4(+)IFNγ(+)-mediated parasite killing in human cutaneous leishmaniasis [published correction appears in J Invest Dermatol 2014;134:2850]. J Invest Dermatol 2013;133:1533–40.

Silveira FT, Lainson R, Corbett CEP. Clinical and immunopathological spectrum of American cutaneous leishmaniasis with special reference to the disease in Amazonian Brazil: a review. Mem Inst Oswaldo Cruz 2004;99:239–51.

SUPPLEMENTARY MATERIALS AND METHODS

Ethics statement

This study was conducted in Mutuípe, Bahia, Brazil, an area where cutaneous leishmaniasis, caused by *Leishmania braziliensis*, is endemic. The present research protocol received approval from the Institutional Review Board of Gonçalo Moniz Institute (IGM-FIOCRUZ) (protocol number 1.673.870/2015-CEP/CPqGM/FIOCRUZ) and from the Brazilian National Ethics Committee (Comissão Nacional de Ética em Pesquisa). Informed written consent was obtained from each participant. All methods were performed in accordance with the guidelines and regulations determined by the Comissão Nacional de Ética em Pesquisa.

Study design and patient enrollment

Individuals diagnosed with disseminated leishmaniasis (DL) were enrolled in the study (n = 7) and subjected to RNA sequencing (RNA-seq) from their lesions. Inclusion criteria consisted of the presence of 10 or more cutaneous acneiform lesions located at two or more body segments and a positive Montenegro Skin Test and/or histopathological examination. Individuals aged ≥18 years were invited to participate. Immunocompromised individuals, individuals who were pregnant, and those who had the presence of atypical disease forms were excluded from the study. Controls for the transcriptome-wide study consisted of healthy skin samples (n = 4) obtained from donors subjected to elective procedures (three male samples from penile foreskin excisions and one female sample from mammoplasty). Skin sample collection resulted in no alterations to surgical procedures, and all the samples were routinely removed according to the originally planned procedure.

Leishmanin skin test

Skin test using *Leishmania* antigen was performed 48–72 hours after intradermal inoculation using a ruler. Inoculation of 1 ml of soluble *Leishmania* antigen (obtained from Fundação Ezequiel Dias, Belo Horizonte, Brazil) was performed using a tuberculin syringe in the anterior face of the right forearm. Results were interpreted on the basis of the area of skin induration, with values smaller than 25 mm^2 considered negative and those greater than 25 mm^2 as positive reactions (Mayrink et al., 1993).

Lesion selection and biopsy procedures

Lesions were selected for biopsy procedures according to their clinical aspect. Biopsy was performed in the border of an active cutaneous lesion (early, elevated, ulcerated, or preulcerated). After local anesthesia with 2% lidocaine, biopsies were collected at the border of DL lesions using a 4-mm punch before the initiation of therapy and were divided into two fragments: one was maintained in formaldehyde and processed for histological analysis, whereas the other was kept in RNAlater (Ambion, Austin, TX) at −70 °C until the time of RNA isolation. Skin biopsies from healthy controls were processed similarly.

RNA isolation and cDNA library preparation

The cryopreserved biopsies were processed into a fine powder using the traditional mortar and pestle system under liquid nitrogen. Total RNA was extracted from these samples using RNeasy Mini Kit (Qiagen, Venlo, The Netherlands), and DNA clean up was performed on the column by DNAse treatment (Qiagen) in accordance with the manufacturer's instructions. RNA was quantified on a NanoDrop spectrophotometer (Nanodrop 1000, Thermo Scientific, Waltham, MA), and RNA integrity was assessed using an Agilent Bioanalyzer (Agilent Technologies, Santa Clara, CA), yielding an RNA integrity number for each sample. One of eight RNA samples of patients with DL were excluded because of low quality (RNA integrity number < 2), and the seven remaining samples had a median RNA integrity number value (±SD) of 7.0 ± 0.25. RNA was frozen at −80 °C until the time of library construction. Ribosomal RNA was depleted from total RNA using the Eukaryote RiboMinus kit (Invitrogen, Carlsbad, CA). RNA-seq libraries were prepared using the Illumina TruSeq Stranded kit (Illumina, San Diego, CA) as per the manufacturer's instructions. Libraries were then sequenced on an Illumina NextSeq500 instrument (Illumina) using the Illumina NextSeq500 High Output kit, producing 150 base pair paired-end reads.

Immunohistochemistry

Immunohistochemistry staining was performed in fresh-frozen specimens obtained by biopsy from four patients with cutaneous leishmaniasis and two with DL. We also selected samples from healthy donors submitted to plastic surgery for aesthetic reasons (Local Human Ethics Committee protocol number 3.334.252). These samples were independent of those that underwent RNA-seq. All samples were embedded in tissue-tek optimal cutting temperature compound (Sakura Finetek USA, Torrance, CA) and snap frozen in liquid nitrogen.

Cryostat-frozen sections, 5 μm thick, were applied to microscope slides and fixed with cold acetone. Staining was performed with rat polyclonal anti-CD4 (catalog number 13573), anti-CD8 (catalog number 59130), or goat polyclonal anti–IL-10 (catalog number 1783) antibodies (Santa Cruz Biotechnology, Dallas, TX), followed by secondary biotinylated anti-rat or anti-goat antibodies (Vector Laboratories, Burlingame, CA). An avidin-biotin-peroxidase system (Vector Laboratories) was used to reveal the reactions, and the slides were counterstained with Mayer's hematoxylin.

Data analysis

Sequences were quality controlled using Trimmomatic, which also allowed for adapter trimming (Bolger et al., 2014). FastQC was used to calculate various read quality metrics (http://www.bioinformatics.babraham.ac.uk/projects/fastqc/). After performing quality control, transcript expression was quantified by the Salmon tool (Patro et al., 2017). For this step, the human reference transcriptome from the GENCODE consortium (release 28) was used to construct a proper index, against which quasimapping was performed (Harrow et al., 2012). Once transcript expression estimates were calculated, gene-level summarization was conducted using the *tximport* package for R (Soneson et al., 2015),

and further gene-level analysis was performed using count-based statistical inference tools. Trimmed mean of M-values normalization was performed to obtain normalization factors across the samples and to account for underlying RNA composition (Robinson and Oshlack, 2010). Before testing for differential expression, low-expression genes (i.e., those having <3 counts per million in at least four samples) were filtered. This threshold was chosen to attain a raw read count of approximately 10 on the basis of the depth of the least sequenced library (Chen et al., 2016). Then, edgeR was used to perform differential expression analysis between the DL samples and the control samples (Robinson et al., 2010). *P*-values were adjusted for multiple hypothesis testing using a false discovery rate (FDR) threshold: genes were considered differentially expressed when FDR-corrected $P \leq 10^{-3}$ and $\log_2$-transformed absolute fold change ≥ 3. Enrichment analysis was performed with DAVID 6.8 (Huang et al., 2009a, 2009b) using the differentially expressed genes as input and the Gene Ontology database as an annotation source. Gene Ontology terms with FDR-corrected $P \leq 0.05$ were considered significant. The REVIGO platform (Supek et al., 2011) was used to remove redundancy in the list of Gene Ontology terms, employing the SimRel semantic similarity measure with a similarity parameter of 0.7. A comparison of DL with other clinical forms of tegumentary disease was also performed using previously published datasets, namely an RNA-seq analysis of diffuse cutaneous leishmaniasis (Christensen et al., 2019) and two localized cutaneous leishmaniasis datasets generated using a microarray (Novais et al., 2015) and RNA-seq (Christensen et al., 2016). For this, all the three previously published datasets, derived from transcriptomic analysis of leishmaniasis skin biopsies compared with those of healthy donors, as well as the present dataset were jointly reanalyzed in the Gene Set Enrichment Analysis framework (Subramanian et al., 2005). Reference gene sets from MSigDB hallmark processes were used during this analysis, derived through the aggregation of multiple MSigDB gene sets to represent well-defined biological states or processes (Liberzon et al., 2015). Gene Set Enrichment Analysis was run in preranked mode, and an ordered gene list was produced per dataset by scoring each gene according to the following formula:

$$\text{score} = -\log_{10}(\text{FDR}) \times \text{sign}(\text{FC}),$$

where FDR is the FDR-corrected *P*-value from the differential expression analysis for a given gene, and FC is the corresponding fold-change value derived from comparisons between infected and control groups. Duplicated probes in the Novais et al. (2015) dataset were collapsed through the maintenance of each gene's maximum score. A total of 1,000 permutations of the gene sets were performed to calculate the FDR, and a cutoff of 0.05 was used to define significance.

To quantify parasite transcripts in DL lesions, HISAT, version 2.1.0 (Kim et al., 2015), was initially used to map the paired-end reads of each sample against the human genome. Alignment parameters were set at default except for the flag –un-conc, which was enforced to obtain reads that failed to align against the host genome. These were then mapped against the genome of *L. braziliensis* MHOM/BR75/M2904 obtained from TriTrypDB, version 45 (https://tritrypdb.org/tritrypdb/) (Aslett et al., 2010). FeatureCounts, version 1.6.3 (Liao et al., 2014), was used to produce a count table summarizing gene-level abundance for each sample, and the corresponding annotation of the *L. braziliensis* genome was obtained in a gene-finding format using TriTrypDB.

To perform digital cytometry, which allowed the estimation of immune cellular fractions from the RNA-seq data of biopsies, quanTIseq was employed (Finotello et al., 2019). This method, specifically developed for RNA-seq data, performs deconvolution of cell fractions on the basis of constrained least-squares regression, yielding estimates for 10 immune cell populations. The quanTIseq bash script was run using default parameters, and boxplots were produced to visually compare cell population estimates across the samples. Owing to multicollinearity in the expression of related cell types, such as regulatory T-cell and nonregulatory CD4+ cells, that hampers their deconvolution (Finotello et al., 2019), we obtained estimates of total CD4+ cells (including regulatory CD4+ cells) by summing the columns regulatory T cells and T-cell CD4 in the quanTIseq output table.

All visualizations were produced in R 3.4.4 (http://www.r-project.org/) using base functions and the packages ggplot2 and circlize (Gu et al., 2014; Wickham, 2010).

SUPPLEMENTARY REFERENCES

Aslett M, Aurrecoechea C, Berriman M, Brestelli J, Brunk BP, Carrington M, et al. TriTrypDB: a functional genomic resource for the Trypanosomatidae. Nucleic Acids Res 2010;38:D457–62.

Bolger AM, Lohse M, Usadel B. Trimmomatic: a flexible trimmer for Illumina sequence data. Bioinformatics 2014;30:2114–20.

Chen Y, Lun AT, Smyth GK. From reads to genes to pathways: differential expression analysis of RNA-Seq experiments using Rsubread and the edgeR quasi-likelihood pipeline. F1000Res 2016;5:1438.

Christensen SM, Dillon LA, Carvalho LP, Passos S, Novais FO, Hughitt VK, et al. Meta-transcriptome profiling of the human-Leishmania braziliensis cutaneous lesion. PLoS Negl Trop Dis 2016;10:e0004992.

Christensen SM, Belew AT, El-Sayed NM, Tafuri WL, Silveira FT, Mosser DM. Host and parasite responses in human diffuse cutaneous leishmaniasis caused by L. amazonensis. PLoS Negl Trop Dis 2019;13:e0007152.

Finotello F, Mayer C, Plattner C, Laschober G, Rieder D, Hackl H, et al. Molecular and pharmacological modulators of the tumor immune contexture revealed by deconvolution of RNA-seq data [published correction appears in Genome Med 29;11:50]. Genome Med 2019;11:34.

Gu Z, Gu L, Eils R, Schlesner M, Brors B. circlize Implements and enhances circular visualization in R. Bioinformatics 2014;30:2811–2.

Harrow J, Frankish A, Gonzalez JM, Tapanari E, Diekhans M, Kokocinski F, et al. GENCODE: the reference human genome annotation for the ENCODE Project. Genome Res 2012;22:1760–74.

Huang da W, Sherman BT, Lempicki RA. Systematic and integrative analysis of large gene lists using DAVID bioinformatics resources. Nat Protoc 2009a;4:44–57.

Huang da W, Sherman BT, Lempicki RA. Bioinformatics enrichment tools: paths toward the comprehensive functional analysis of large gene lists. Nucleic Acids Res 2009b;37:1–13.

Kim D, Langmead B, Salzberg SL. HISAT: a fast spliced aligner with low memory requirements. Nat Methods 2015;12:357–60.

Liao Y, Smyth GK, Shi W. featureCounts: an efficient general purpose program for assigning sequence reads to genomic features. Bioinformatics 2014;30:923–30.

Liberzon A, Birger C, Thorvaldsdóttir H, Ghandi M, Mesirov JP, Tamayo P. The molecular signatures database hallmark gene set collection. Cell Syst 2015;1:417–25.

Mayrink W, Melo MN, Costa CA, Coutinho SG, Hermeto MV, Genaro O, et al. Multinational development of a standard skin test antigen in America: preliminary results in the Minas Gerais State, Brazil. Mem Inst Oswaldo Cruz 1993;88(Suppl.):226.

Novais FO, Carvalho LP, Passos S, Roos DS, Carvalho EM, Scott P, et al. Genomic profiling of human Leishmania braziliensis lesions identifies transcriptional modules associated with cutaneous immunopathology. J Invest Dermatol 2015;135:94–101.

Patro R, Duggal G, Love MI, Irizarry RA, Kingsford C. Salmon provides fast and bias-aware quantification of transcript expression. Nat Methods 2017;14:417–9.

Robinson MD, McCarthy DJ, Smyth GK. edgeR: a Bioconductor package for differential expression analysis of digital gene expression data. Bioinformatics 2010;26:139–40.

Robinson MD, Oshlack A. A scaling normalization method for differential expression analysis of RNA-seq data. Genome Biol 2010;11:R25.

Soneson C, Love MI, Robinson MD. Differential analyses for RNA-seq: transcript-level estimates improve gene-level inferences. F1000Res 2015;4:1521.

Subramanian A, Tamayo P, Mootha VK, Mukherjee S, Ebert BL, Gillette MA, et al. Gene set enrichment analysis: a knowledge-based approach for interpreting genome-wide expression profiles. Proc Natl Acad Sci USA 2005;102:15545–50.

Supek F, Bošnjak M, Škunca N, Šmuc T. REVIGO summarizes and visualizes long lists of Gene Ontology terms. PLoS One 2011;6:e21800.

Wickham H. ggplot2: elegant graphics for data analysis. New York: Springer; 2010.

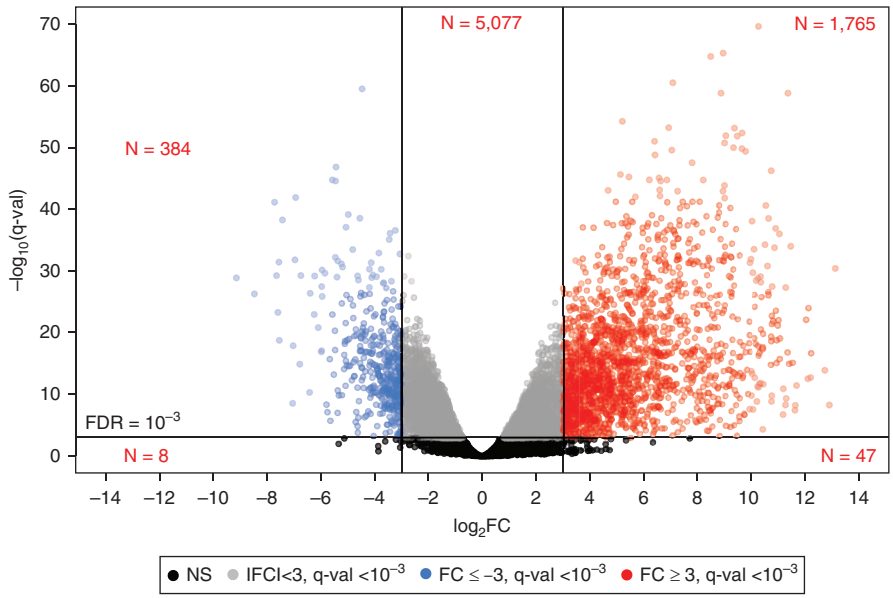

Supplementary Figure S1. Volcano plot showing differentially expressed genes in DL versus those in healthy skin biopsies. Each dot represents a gene, and colors denote genes that were not found differentially expressed (black dots), were significant on the basis of q-value but with $\log_2$FC in the [−3, 3] interval (gray dots), were significantly upregulated (red dots), or were significantly downregulated (blue dots). The number of genes in a given class is shown in red at the corresponding quadrant, except those that did not reach statistical significance nor reached a minimum FC deviation. q-value denotes the FDR-adjusted *P*-value. DL, disseminated leishmaniasis; FC, fold change; FDR, false discovery rate; val, value.

Supplementary Figure S2. Enriched and depleted biological processes in DL. (**a**) A total of 49 processes were significantly enriched in DL compared with those in the healthy skin samples. Circle size is proportional to the number of genes in each respective process, and color varies according to the degree of enrichment and/or depletion (hypergeometric test). (**b, c**) Detailed hierarchical view of the (**b**) enriched and (**c**) depleted processes, with related terms grouped in same-colored rectangles. Rectangle size reflects process enrichment. Summarization was performed using REVIGO (see Supplementary Material and Methods). DL, disseminated leishmaniasis; ERK, extracellular signal–regulated kinase; GTPase, guanosine triphosphatase.

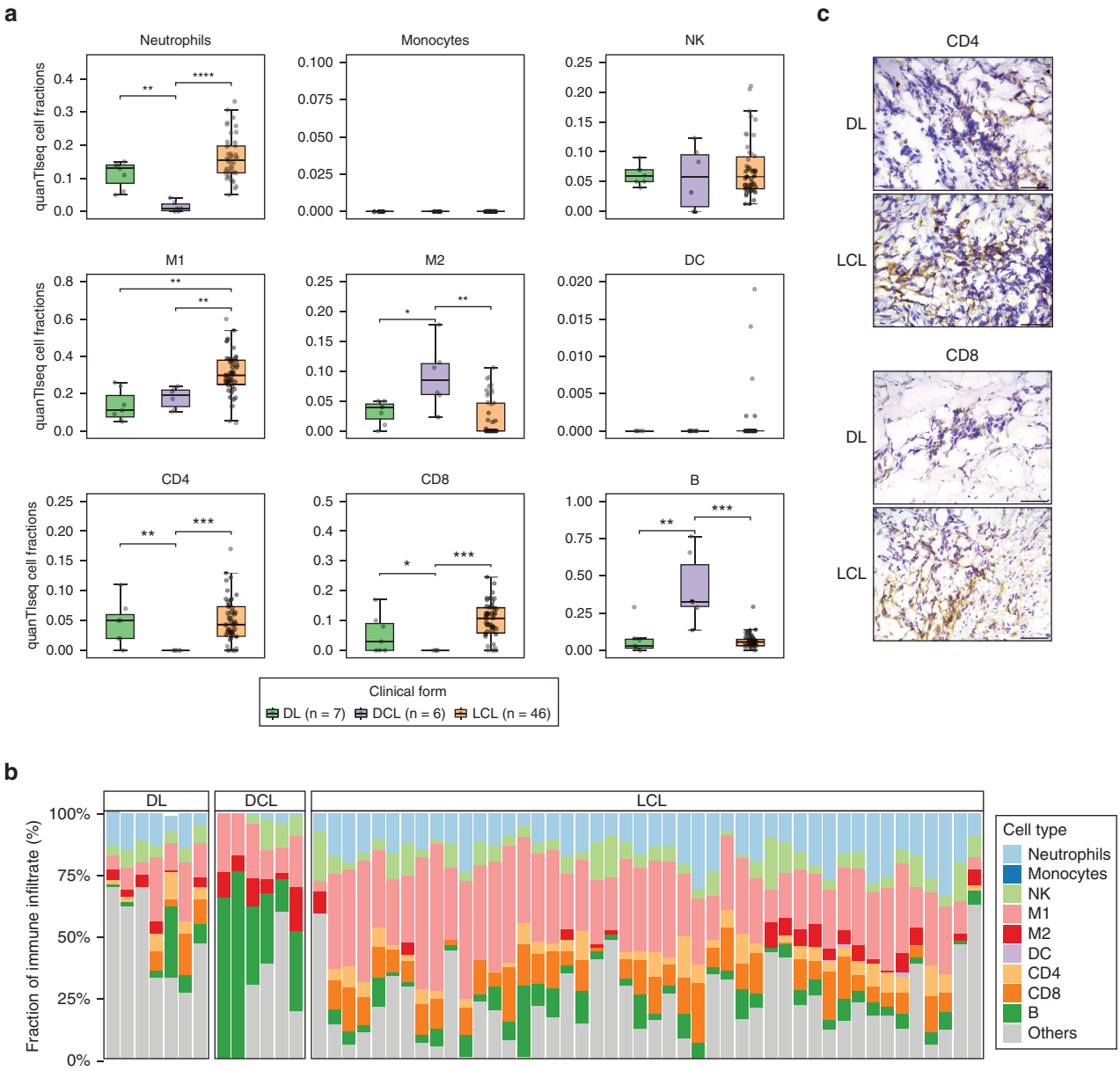

Supplementary Figure S3. Digital cytometry of DL, DCL, and LCL lesions shows evidence of unique patterns within each clinical form as well as marked interindividual differences. quanTIseq was used to perform digital cytometry using RNA-seq data. The fractions of predicted immune infiltrate were compared across the lesions of DL (this work), DCL (work by Christensen et al. [2019]), and LCL (works by Amorim et al. [2019] and Christensen et al. [2016]). (**a**) Summarization of the results of immune cell populations shown as boxplots. Overlaid black points represent cell population estimates in individual samples. Mann–Whitney *U* test was applied to compare the groups. $*P < 0.05$, $**P < 0.01$, $***P < 0.001$, $****P < 0.0001$. B indicates B cells, CD4 indicates total $CD4^+$ T cells (also including $CD4^+$ regulatory T cells), and CD8 indicates $CD8^+$ T cells. (**b**) Individual composition of the predicted immune infiltrates in each analyzed skin lesion. (**c**) Immunohistochemical staining of $CD4^+$ and $CD8^+$ cells in biopsy samples from skin lesions of patients with DL or those with LCL, counterstained with hematoxylin. Magnification ×40, Bar = 50 μm. DC, dendritic cell; DCL, diffuse cutaneous leishmaniasis; DL, disseminated leishmaniasis; LCL, localized cutaneous leishmaniasis; M1, M1 macrophages; M2, M2 macrophages; RNA-seq, RNA sequencing.